MITSUBISHI ELECTRIC RESEARCH LABORATORIES
http://www.merl.com

Extremum Seeking-based Parameter Identification for State-of-Power Prediction of Lithium-ion Batteries

Benosman, Mouhacine; Wei, Chun

TR2016-143 November 20, 2016

Abstract

Accurate state-of-power (SOP) estimates are critical for building battery systems with optimized performance and longer life in electric vehicles (EVs) and hybrid electric vehicles (HEVs). This paper proposes a novel parameter identification method and its implementation on SOP prediction for lithium-ion batteries. The extremum seeking algorithm is developed for identifying the parameters of batteries on the basis of an electrical circuit model incorporating hysteresis effect. The estimated battery parameters can then be used for online stage -of-charge, state-of-health, and SOP estimation for lithium-ion batteries. In addition, based on the electrical circuit model with the identified parameters, a battery SOP prediction algorithm is derived, which considers both the voltage and current limitations of the battery. The proposed method is suitable for real operation of embedded battery management system (BMS) due to its low complexity and numerical stability. Simulation results for lithium-ion batteries are provided to validate the proposed parameter identification and SOP prediction methods.

IEEE International Conference on Renewable Energy Research and Applications

Extremum Seeking-based Parameter Identification for State-of-Power Prediction of Lithium-ion Batteries

Abstract—**Accurate state-of-power (SOP) estimates are critical for building battery systems with optimized performance and longer life in electric vehicles (EVs) and hybrid electric vehicles (HEVs). This paper proposes a novel parameter identification method and its implementation on SOP prediction for lithium-ion batteries. The extremum seeking algorithm is developed for identifying the parameters of batteries on the basis of an electrical circuit model incorporating hysteresis effect. The estimated battery parameters can then be used for online stage-of-charge, state-of-health, and SOP estimation for lithium-ion batteries. In addition, based on the electrical circuit model with the identified parameters, a battery SOP prediction algorithm is derived, which considers both the voltage and current limitations of the battery. The proposed method is suitable for real operation of embedded battery management system (BMS) due to its low complexity and numerical stability. Simulation results for lithium-ion batteries are provided to validate the proposed parameter identification and SOP prediction methods.**

Index Terms—**Battery management system, extremum seeking, lithium-ion battery, parameter identification, state-of-power.**

I. Introduction

Electric vehicle (EV) and hybrid electric vehicle (HEV) are two promising solutions to relief the energy crisis and environmental issues raised by the oil-dependent vehicles [1]. The core component of the EV and HEV is the battery system. Lithium-ion batteries have been widely used in EVs and HEVs due to their high energy and power densities and long cycle life [2]. However, effective battery management system (BMS) is still a remarkable challenge and necessity to guarantee the reliable and safe battery operations. The critical function of the BMS is to estimate the state-of-charge (SOC), state-of-health (SOH), and state-of-power (SOP) of the battery system in real-time. Due to the absence of sensors for direct measurements of these quantities, battery models are used to estimate these states based on model-based estimation methods. To improve the SOC, SOH, and SOP estimation accuracy of lithium-ion batteries, the parameters of the battery model should be identified effectively.

Kalman filter (KF)-based methods and linear least square regression-based methods are two main types of real-time battery parameter identification methods. Various types of KF have been proposed, such as linear KF [3], extended KF [4], dual extended KF [5], to estimate the parameters and the states of the battery model simultaneously. Although accurate solutions can be obtained by using KF-based methods, they cause high computational complexity and may be difficult to implement in real-time embedded systems. Compared to the KF-based methods, the least squares methods are more computationally competitive without losing much accuracy. Thus, they are most widely used methods to estimate parameters of a battery model so far. Various least square-based methods have been proposed, such as recursive least square [6], and moving window least square [7], to perform online estimation of battery parameters.

The estimation of the peak power capability of the battery is essential to determine the maximum available power for acceleration and regenerating braking of the EV and HEV, thus avoiding over-charging or over-discharging the battery. SOP is the parameter to describe the maximum charging and discharging capabilities of the battery [8]. Accurate SOP estimation can guarantee optimum performance and longer life of the battery. A dynamic electrochemical polarization model is proposed in [9], and the battery SOP for the next sampling time is accurately estimated based on this model. An adaptive extended KF is proposed to estimate the SOC and SOP simultaneously in [10], which realizes a long term SOP estimation. However, only the voltage limitation is considered in the above researches when calculating the peak power capability, the battery current limitation is ignored.

This paper proposes a novel parameter identification method and its implementation on SOP prediction for lithium-ion batteries. The extremum seeking (ES) algorithm [11]-[12] is developed for identifying the parameters of the battery model based on an electrical circuit model incorporating hysteresis effect. The convergence of the ES algorithm for battery parameter identification is proved. The estimated battery parameters can then be used for online SOC, SOH, and SOP estimation for lithium-ion batteries. In this paper, based on the electrical circuit model with the identified parameters, a battery SOP prediction algorithm is derived, which considers both the voltage and current limitations of the battery. The proposed method is suitable for real operation of embedded battery management system (BMS) due to its low complexity and numerical stability. Simulation results for lithium-ion batteries are provided to validate the proposed parameter identification and SOP prediction methods.

II. The Battery Model

The battery model should be carefully chosen to ensure a precise estimation of states and parameters. For real-time application in embedded systems, a balance between the accuracy and complexity of the battery model should be made. Electrical circuit battery models are the most suitable for embedded applications due to their low complexity and the ability of characterizing the current-voltage (I-V) dynamics of battery cells [13]. The voltage hysteresis effect between the charging and discharging widely exists in Li-ion batteries, especially for the $LiFePO_4$-type. It is demonstrated that the first-order resistor-capacitor (RC) model with one-state hysteresis seems to be the best choice for $LiFePO_4$ cells [14]. Therefore, the first-order RC model with a hysteresis, as shown in Fig. 1, is used in this paper to provide a good balance between model accuracy and complexity.

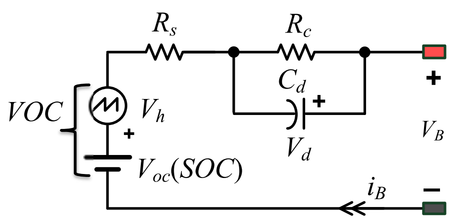

Fig. 1. The first-order RC model with hysteresis.

As shown in Fig. 1, the open-circuit voltage (OCV) V_{oc} includes two parts. The first part, $V_{oc}(SOC)$, represents the equilibrium OCV as a function of the SOC. The second part V_h is the hysteresis voltage to capture the hysteresis behavior of the OCV curves. The RC circuit models the I-V characteristics and the transient response of the battery cell. The series resistance, R_s, is used to describe the charge/discharge energy loss in the cell; the charge transfer resistance, R_c, and double layer capacitance, C_d, are used to characterize the charge transfer and short-term diffusion voltage, V_d, of the cell; V_B represents the terminal voltage of the cell.

The following voltage hysteresis model is used [15]:

$$\frac{\partial V_h}{\partial t} = -\rho(\eta i_B - \nu S_D)[V_{h\max} + sign(i_B)V_h], \quad (1)$$

where ρ is the hysteresis parameter representing the convergence rate, η is the Coulomb efficiency (assuming η =1), i_B is the instantaneous current applied to the battery, ν is the self-discharge multiplier for hysteresis expression, S_D is the self-discharge rate, and $V_{h\max}$ is the maximum hysteresis voltage. The model (1) describes the dependency of the hysteresis voltage V_h on the current, self-discharge, and hysteresis boundaries. The parameter ρ is chosen to minimize the voltage error between the V_{OC}-SOC curves from simulation and experiments, respectively.

A discrete-time battery model, including the electrical circuit model and the hysteresis model, can be written as follows

$$X(k+1) = \begin{bmatrix} 1 & 0 & 0 \\ 0 & \gamma & 0 \\ 0 & 0 & H \end{bmatrix} X(k) + \begin{bmatrix} -\frac{\eta T_s}{C_{\max}} & 0 \\ R_c(1-\gamma) & 0 \\ 0 & (H-1)sign(i_B) \end{bmatrix} \begin{bmatrix} i_B(k) \\ V_{h\max} \end{bmatrix},$$

$$y(k) = V_B(k) = V_{OC}(SOC(k)) - V_d(k) - R_s i_B(k) + V_h(k),$$

$$V_{OC}(SOC) = b_0 \exp(-b_1 SOC) + b_2 + b_3 SOC - b_4 SOC^2 + b_5 SOC^3, \quad (2)$$

where $X(k+1) = \begin{bmatrix} SOC(k+1) & V_d(k+1) & V_h(k+1) \end{bmatrix}^T$ is the state, $y(k)$ is the measured output, k is the time index, $C_{\max}$ denotes the maximum capacity of the battery, T_s is the sampling period, $\gamma = \exp(\frac{-T_s}{\tau})$ with $\tau = R_c C_d$, $H(i_B) = \exp(-\rho|i_B|T_s)$, and b_j for $0 \le j \le 5$ are the coefficients used to parameterize the V_{OC}-SOC curve. Coefficients b_j for $0 \le j \le 5$ can be extracted by pulsed current tests or constant charge and discharge current test using a small current to minimally excite transient response of the battery cell [16].

III. ES-Based Parameter Identification of Lithium-Ion Battery

A. Basics of ES

The basic scheme for a single gradient-based ES algorithm is shown in Fig. 2. The algorithm injects a sinusoidal perturbation $a\sin\omega t$ into the system, resulting in an output of the cost function $Q(\theta)$. This output $Q(\theta)$ is subsequently multiplied by $a\sin\omega t$. The resulting signal after multiplying a gain l, $\dot{\xi}$, is an estimate of the gradient of the cost function with respect to θ, i.e., the optimization vector. The gradient estimate is then passed through an integrator $1/s$ and added to the modulation signal $a\sin\omega t$. The corresponding equations for the basic multi-parameter ES algorithm are:

$$\dot{\xi}_i = a_i l \sin(\omega_i t) Q(\theta), \quad (3)$$

$$\theta_i = \xi_i + a_i \sin(\omega_i t), \quad (4)$$

where $\omega_i \neq \omega_j$, $\omega_i + \omega_j \neq \omega_k$, $i, j, l, \in \{1, 2, n\}$, and $\omega_i > \omega^*$, with ω^* large enough to ensure the convergence. If the parameters a_i, ω_i, and l are properly selected, the cost function output $Q(\theta)$ will converge to an neighborhood of the optimal cost function value $Q(\theta^*)$.

In order to implement the ES algorithm in the real-time embedded system, a discrete version of the ES algorithm is required. The discrete version of the ES algorithm is given:

$$\xi_i(k+1) = \xi_i(k) + a_i l \Delta T \sin(\omega_i k) Q(\theta(k)), \quad (5)$$

$$\theta_i(k+1) = \xi_i(k+1) + a_i \sin(\omega_i(k)), \quad (6)$$

where k is the time step and ΔT is the sampling time.

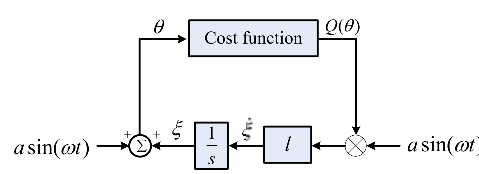

Fig. 2. Block diagram of the basic gradient-based extremum seeking algorithm.

B. ES for Parameter Identification

The multi-parameter ES algorithm, e.g., [12], is used to identify the parameters of the battery model, i.e., R_s, R_c, C_d, and $C_{\max}$ in (2). The block diagram of ES-based parameter identification method for lithium-ion battery is shown in Fig. 3. At each time step, a battery terminal voltage V_B can be measured under a specific operating current i_B. The measured V_B is compared with the estimated battery terminal voltage $\hat{V}_B$, which is obtained from the battery model based on the measured current i_B using the estimated battery model parameters. The error of V_B and $\hat{V}_B$ is used to generate a cost function, which represents the convergence of the battery parameters. The battery parameters will then be updated by the ES algorithm and used to generate a new $\hat{V}_B$ in the next time step. The parameter updating process will proceed until the cost function reaches to a small criterion or the algorithm reaches the maximum iteration number.

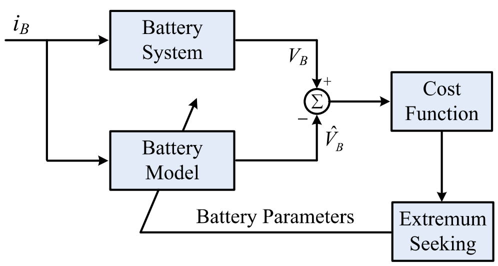

Fig. 3. Extremum seeking-based parameter identification method for lithium-ion battery.

Using the estimated parameters $\theta = [\ \hat{R}_s,\ \hat{R}_c,\ \hat{C}_d,\ \hat{C}_{\max}\ ]^T$, the battery model (2) can be written as

$$S\hat{O}C(k+1) = S\hat{O}C(k) - \frac{\eta T_s}{\hat{C}_{\max}} i_B(k),$$

$$\hat{V}_d(k+1) = \gamma(k)\hat{V}_d(k) + \hat{R}_c(k)(1-\gamma)i_B(k),$$

$$\hat{V}_h(k+1) = H\hat{V}_h(k) + (H-1)sign(i_B(k))V_{h\max},$$

$$\hat{V}_B(k) = V_{OC}(S\hat{O}C(k)) - \hat{V}_d(k) - \hat{R}_s(k)i_B(k) + \hat{V}_h(k), \quad (7)$$

where $\gamma(k) = \exp(\frac{-T_s}{\tau(k)})$, and $\tau(k) = \hat{R}_c(k)\hat{C}_d(k)$.

The following cost function is defined for each iteration:

$$Q(\theta(k)) = K_p \int_{t_0}^{T} [V_B(t) - \hat{V}_B(t)]^2 dt, \quad (8)$$

where T- t_0 represents the time interval over which the ES learning cost function is evaluated, and K_p is a gain.

The battery model parameters are updated in the following form:

$$\hat{R}_s(k+1) = R_{s,nominal} + \delta\hat{R}_s(k),$$

$$\hat{R}_c(k+1) = R_{c,nominal} + \delta\hat{R}_c(k),$$

$$\hat{C}_d(k+1) = C_{d,nominal} + \delta\hat{C}_d(k),$$

$$\hat{C}_{\max}(k+1) = C_{\max,nominal} + \delta\hat{C}_{\max}(k), \quad (9)$$

where $R_{s,nominal}$, $R_{c,nominal}$, $C_{d,nominal}$, and $C_{\max,nominal}$ are the nominal initial values of the battery model parameters. Following (5) and (6), the variations of the identified battery model parameters are given by

$$\xi_1(k+1) = \xi_1(k) + a_1 l \Delta T \sin(\omega_1 k) Q(\theta(k)),$$

$$\delta\hat{R}_s(k) = \xi_1(k+1) + a_1 \sin(\omega_1(k)),$$

$$\xi_2(k+1) = \xi_2(k) + a_2 l \Delta T \sin(\omega_2 k) Q(\theta(k)),$$

$$\delta\hat{R}_c(k) = \xi_2(k+1) + a_2 \sin(\omega_2(k)),$$

$$\xi_3(k+1) = \xi_3(k) + a_3 l \Delta T \sin(\omega_3 k) Q(\theta(k)),$$

$$\delta\hat{C}_d(k) = \xi_3(k+1) + a_3 \sin(\omega_3(k)),$$

$$\xi_4(k+1) = \xi_4(k) + a_4 l \Delta T \sin(\omega_4 k) Q(\theta(k)),$$

$$\delta\hat{C}_{\max}(k) = \xi_4(k+1) + a_4 \sin(\omega_4(k)), \quad (10)$$

where a_1, a_2, a_3, and a_4 are positive and $\omega_p \neq \omega_q, \omega_p + \omega_q \neq \omega_r$, $p, q, r \in \{1,2,3,4\}$, for $p \neq q \neq r$.

C. Convergence Analysis

To be able to write a formal convergence analysis, we first need to introduce the following assumptions.

Assumption 1: The ES cost function Q has a local minimum at the true parameter values $\theta^* = [\ \hat{R}_s,\ \hat{R}_c,\ \hat{C}_d,\ \hat{C}_{\max}\ ]^T$.

Assumption 2: The original parameters estimates vector, i.e., the nominal parameters value, is close enough to the actual parameters vector.

Assumption 3: The cost function is analytic and its variation with respect to the uncertain variables is bounded in the neighborhood of θ^*.

We summarize the convergence of the ES estimation algorithm in the following Lemma.

Lemma 1. The ES estimation algorithm (8), (9), and (10), under assumptions 1, 2, 3, where the dither frequencies ω_p, $p \in \{1,2,3,4\}$ are such that $\omega_p > \omega^*$, with ω^* large enough, asymptotically converges to the true values, with the estimation upper-bound

$$||\hat{\theta} - \theta^*|| \leq \frac{\varepsilon_1}{\omega_0} + \sqrt{\sum_{i=1}^{i=4} a_i^2},$$

where $\varepsilon_1 > 0$, and $\omega_0 = \max\{\omega_1, \ldots, \omega_4\}$.

Proof. Due to space limitation, we refer the reader to [12] where a proof of convergence for this type of ES algorithms can be found.

IV. SOP Estimation

To guarantee the safe and durable operation, the working current and voltage of the lithium-ion battery should be restricted in a range so that the battery power will be limited by the minimum value of the two restrictions given by

$$SOP_{discharge} = \min[SOP^{V}_{discharge}\ SOP^{I}_{discharge}],$$
$$SOP_{charge} = \max[SOP^{V}_{charge}\ SOP^{I}_{charge}], \quad (11)$$

where $SOP_{discharge}$ and SOP_{charge} are the maximum discharging and charging capabilities of the battery, respectively, $SOP^{V}_{discharge}$ and SOP^{V}_{charge} are the battery SOPs under voltage limitation, $SOP^{I}_{discharge}$ and SOP^{I}_{charge} are the battery SOPs under current limitation.

A. SOP Based on Voltage Limitation

In order to predict the maximum power capability under the voltage limitation, (7) is rewritten into

$$S\hat{O}C(k+1) = S\hat{O}C(k) - \frac{\eta T_s}{C_{\max}} i_B(k),$$
$$\hat{V}_d(k+1) = \gamma \hat{V}_d(k) + R_c(1-\gamma) i_B(k),$$
$$\hat{V}_h(k+1) = H\hat{V}_h(k) + (H-1)sign(i_B(k))V_{h\max},$$
$$\hat{i}_B(k+1) = (V_{OC}(S\hat{O}C(k+1)) - \hat{V}_d(k+1) + \hat{V}_h(k+1) - V_B(k+1)) / R_s \quad (12)$$

where the battery model parameters R_s, R_c, C_d, and $C_{\max}$ have been identified by the ES algorithm. The estimated current for the next time step $\hat{i}_B(k+1)$ can be obtained with a given $V_B(k+1)$. According to (12), the maximum discharging and charging current can be obtained by setting $V_B(k+1)$ to the minimum and maximum limiting value. Then, the battery SOP can be obtained by multiplying the maximum discharging and charging current with the limiting voltage,

$$SOP^{V}_{discharge}(k+1) = V_{B\min}\hat{i}_B(k+1)(V_{B\min}),$$
$$SOP^{V}_{charge}(k+1) = V_{B\max}\hat{i}_B(k+1)(V_{B\max}), \quad (13)$$

where $SOP^{V}_{discharge}(k+1)$ and $SOP^{V}_{charge}(k+1)$ are the maximum discharging and charging capabilities for the next sampling interval under the voltage limitation, $V_{B\max}$ and $V_{B\min}$ are the maximum and minimum voltage allowed for the battery operation, respectively. With the updated $i_B(k)$ and $V_B(k)$, the algorithm above can periodically predict the SOP of the battery for the next time step.

B. SOP Based on Current Limitation

The maximum charging and discharging currents of the battery are also limited and should be considered in the SOP estimation. In order to predict the maximum power capability under the current limitation, (7) is rewritten into

$$S\hat{O}C(k+1) = S\hat{O}C(k) - \frac{\eta T_s}{C_{\max}} i_B(k),$$
$$\hat{V}_d(k+1) = \gamma \hat{V}_d(k) + R_c(1-\gamma) i_B(k),$$
$$\hat{V}_h(k+1) = H\hat{V}_h(k) + (H-1)sign(i_B(k))V_{h\max},$$
$$\hat{V}_B(k+1) = V_{OC}(S\hat{O}C(k+1)) - \hat{V}_d(k+1) - R_s i_B(k+1) + \hat{V}_h(k+1) \quad (14)$$

where the battery model parameters R_s, R_c, C_d, and $C_{\max}$ have been identified by the ES algorithm. The estimated voltage for the next time step $\hat{V}_B(k+1)$ can be obtained with a given $i_B(k+1)$.

According to (14), by setting $i_B(k+1)$ to the maximum discharging current $I_{\max}$ or maximum charging current $I_{\min}$, $\hat{V}_B(k+1)$ can be calculated. Then, the battery SOP can be expressed as

$$SOP^{I}_{discharge}(k+1) = I_{B\max}\hat{V}_B(k+1)(I_{B\max}),$$
$$SOP^{I}_{charge}(k+1) = I_{B\min}\hat{V}_B(k+1)(I_{B\min}), \quad (13)$$

where $SOP^{I}_{discharge}(k+1)$ and $SOP^{I}_{charge}(k+1)$ are the maximum discharging and charging capabilities for the next sampling interval under the current limitation, $I_{\max}$ and $I_{\min}$ are the maximum discharging and charging currents allowed for the battery operation, respectively. With the updated $i_B(k)$ and $V_B(k)$, the algorithm above can periodically predict the SOP of the battery under the current limitation for the next time step.

V. Simulation Results

Simulations are carried out in Matlab to validate the proposed ES-based parameter identification method and the SOP prediction algorithm for a Li-ion battery. Two different types of current profile are applied to test the battery model: high pulse current cycle and the current profile which is proportional to the speed profile in the standard Urban Dynamometer Driving Schedule (UDDS). Due to space limitation, we only report here the first set of tests. The battery model is first tested under a high pulse current cycle (i_B=10C, see Fig. 4(a)). This current profile leads to an output voltage profile shown in Fig. 4(b) from the battery model. Table I lists the values of the model parameters, which are based on a polymer Li-ion battery cell [13] with the maximum capacity scaled up to 10 Ah. The initial estimated states is $[SOC(0), V_d(0), V_h(0)]^T = [0.35, 0, 0]^T$. The initial values for the battery model parameters R_s, R_c, C_d, and $C_{\max}$ are 0.03, 0.06, 3000, and 5, respectively. The estimation algorithm (8), (9), and (10) was implemented with a_1=10, a_2=35, a_3=16, a_4=0.8, ω_1 =1e-4, ω_2 =5e-4, ω_3 =10, ω_4 =2e-4. Fig. 4(c)-(f) show the results of the parameter identification by the proposed ES-based method. The battery model parameters converge to their true values well after a certain number of iterations. Fig. 4(g) shows the cost function during this process. The cost function decreases to a small value after the battery parameters converge, which indicates the estimated terminal voltage $\hat{V}_B$ from the battery model converges to the true value V_B.

After the estimated battery parameters converge, their final values are used for the SOP prediction of the battery. Fig. 5 shows the results of the SOP prediction, in which positive power means discharging and negative power means charging. Three curves are provided in Fig. 5, which are the SOP prediction using the initial, final and true values of the battery model parameters, respectively. It can be clearly observed that by using the estimated battery parameters obtained from the ES-based method, the predicted SOP overlaps with the true SOP of the battery well. SOP prediction using the estimated parameters shows a high accuracy. Fig. 5 also shows that even a small divergence of the battery parameters will cause a large error of the predicted SOP, which indicates the importance of the battery parameter identification with high accuracy.

TABLE I. SIMULATED BATTERY MODEL PARAMETERS

$C_{\max}$	10 Ah	C_d	4000F	R_s	0.06Ω	R_c	0.02 Ω
$V_{h\max}$	0.01V	ρ	2.47e-4	a_0	-0.852	a_1	63.867
a_2	3.692	a_3	0.559	a_4	0.51	a_5	0.508

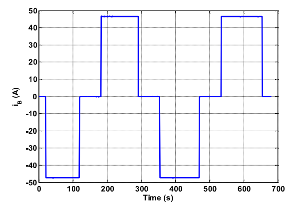

(a)

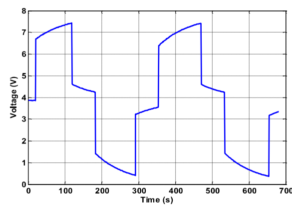

(b)

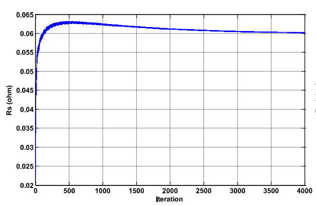

(c)

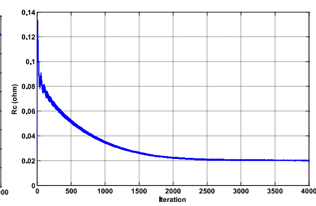

(d)

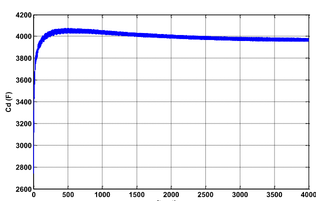

(e)

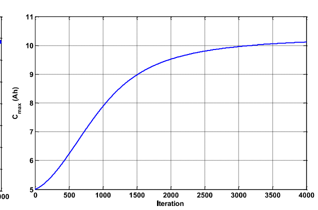

(f)

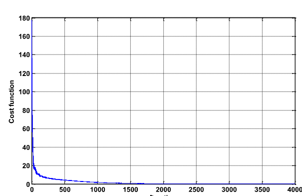

(g)

Fig. 4. Simulation results of ES-based parameter identification of for a Li-ion battery under high pulse current cycle: (a) input current profile; (b) cell voltage; (c) estimated R_s; (d) estimated R_c; (e) estimated C_d; (f) estimated C_{max}; and (g) cost function.

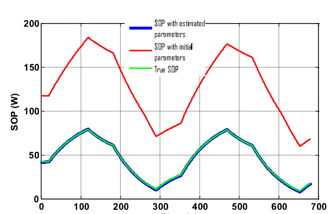

(a)

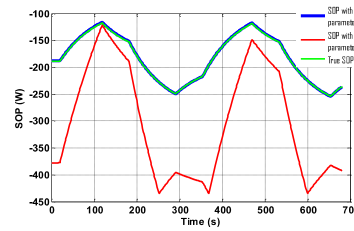

(b)

Fig. 5. SOP estimation: (a) for discharge; and (b) for charge (red-line: before estimation, blue-line: after estimation, green-line: true value).

VI. Conclusion

We have proposed a novel parameter identification method and its application to SOP prediction for lithium-ion batteries. The ES algorithm has been developed for identifying the parameters of batteries on the basis of an electrical circuit model incorporating hysteresis effect. Based on the electrical circuit model with the identified parameters, a battery SOP prediction algorithm has been developed, which considers voltage and current limitations of the battery. Simulation results for lithium-ion batteries have been provided to validate the proposed approach.

References

[1] G. Plett, "Extended Kalman filtering for battery management systems of LiPB-based HEV battery packs- Part 1. Background," *J. Power Sources*, vol. 134, no. 2, pp. 252-261, 2004.

[2] Y. H. Chiang, W. Y. Sean, and J. C. Ke, "Online estimation of internal resistance and open-circuit voltage of lithium-ion batteries in electric vehicles," *J. Power Sources*, vol. 196, no. 8, pp. 3921-3932, 2011.

[3] L. W. Juang, P. J. Kollmeyer, and R. D. Lorenz, "Implementation of online battery state-of-power and state-of-function estimation in electric vehicle applications," *in Proc. IEEE Energy Conversion Congress and Exposition*, Sep. 15-20, pp. 3491-3497, 2012.

[4] G. Plett, "Extended Kalman filtering for battery management systems of LiPB-based HEV battery packs - Part 3. State and parameter estimation," *J. Power Sources*, vol. 134, no. 2, pp. 262-276, 2004.

[5] G. Plett, "Sigma-point Kalman filtering for battery management systems of LiPB-based HEV battery packs: Part 2. Simultaneous state and parameter estimation," *J. Power Sources*, vol. 161, pp. 1369-1384, 2006.

[6] M. A. Roscher, O. S. Bohlen, and D. U. Sauer, "Reliable state estimation of multicell lithium-ion battery system," *IEEE Trans. Energy Conv.*, vol. 26, no. 3, pp. 737-743, 2011.

[7] C. R. Gould, C. M. Bingham, D. A. Stone, and P. Bentley, "New battery model and state-of-health determination through subspace parameter estimation and state-observer techniques," *IEEE Trans. Vehicular Tech.*, vol. 58, no., 8, pp. 3905-3916, 2009.

[8] T. Feng, L. Yang, X. Zhao, H. Zhang, and J. Qiang, "Online identification of lithium-ion battery parameters based on an improved equivalent-circuit model and its implementation on battery state-of-power prediction," *J. Power Sources*, vol. 281, pp. 192-203, 2015.

[9] F. Sun, R. Xiong, H. He, W. Li, and JEE Aussems, "Model-based dynamic multi-parameter method for peak power estimation of lithium-ion batteries," *Applied Energy*, vol. 96, pp. 378-386, 2012.

[10] R. Xiong, H. He, F. Sun, X. Liu, and Z. Liu, "Model-based state-of-charge and peak power capability joint estimation fo lithium-ion battery in plug-in hybrid electric vehicles," *J. Power Sources*, vol. 229, pp. 159-169, 2013.

[11] M. Benosman, and G. M. Atinc, "Multi-parametric extremum seeking-based learning control for electromagnetic actuators," in *Proc. American Control Conference (ACC)*, pp. 1914-1919, 2013.

[12] M. Benosman, "Extremum seeking-based indirect adaptive control and feedback gains auto-tuning for nonlinear systems," available online: http://www.merl.com/publications/docs/TR2015-009.pdf.

[13] T. Kim, and W. Qiao, "A hybrid battery model capable of capturing dynamic circuit characteristics and nonlinear capacity effects," *IEEE Trans. Energy Conv.*, vol. 26, no. 4, pp. 1172-1180, 2011.

[14] X. Hu, S. Li, and H. Peng, "A comparative study of equivalent circuit models for Li-ion batteries," *J. Power Sources*, vol. 198, pp. 359-367, 2012.

[15] M. Verbrugge, and E. Tate, "Adaptive state of charge algorithm for nickel metal hydride batteries including hysteresis phenomena," *J. Power Sources*, vol. 126, pp. 236-249, 2004.

[16] G. Plett, "Results of temperature-dependent LiPB cell modeling for HEV SOC estimation," *in Proc. The 21st Electric Vehicle Symposium*, Monaco, 2005.